European Journal of Medicinal Chemistry 68 (2013) 212–221

Contents lists available at ScienceDirect

European Journal of Medicinal Chemistry

journal homepage: http://www.elsevier.com/locate/ejmech

Original article

Synthesis, molecular docking and kinetic properties of β-hydroxy-β-phenylpropionyl-hydroxamic acids as *Helicobacter pylori* urease inhibitors

Zhu-Ping Xiao [a,*], Zhi-Yun Peng [a], Jing-Jun Dong [b], Rui-Cheng Deng [a], Xu-Dong Wang [a], Hui Ouyang [a], Pan Yang [a], Juan He [a], Yuan-Feng Wang [a], Man Zhu [a], Xiao-Chun Peng [a], Wan-Xi Peng [a,c,**], Hai-Liang Zhu [a,b,***]

[a] College of Chemistry and Chemical Engineering, Key Laboratory of Hunan Forest Products and Chemical Industry Engineering, Jishou University, Jishou 416000, PR China
[b] State Key Laboratory of Pharmaceutical Biotechnology, Nanjing University, Nanjing 210093, PR China
[c] School of Materials Science and Engineering, Central South University of Forestry and Technology, Changsha 410004, PR China

ARTICLE INFO

Article history:
Received 31 March 2013
Received in revised form
3 July 2013
Accepted 5 July 2013
Available online 9 August 2013

Keywords:
Hydroxamic acid
Helicobacter pylori urease
Inhibitor
A mixture of competitive and uncompetitive mechanism

ABSTRACT

Inhibition of urease results in *Helicobacter pylori* growth arrest in the stomach, promoting urease as promising targets for gastrointestinal ulcer therapy. Twenty hybrid derivatives of flavonoid scaffold and hydroxamic acid, β-hydroxy-β-phenylpropionylhydroxamic acids, were therefore synthesized and evaluated against *H. pylori* urease. Biological evaluation of these compounds showed improved urease inhibition exhibiting micromolar to mid-nanomolar IC_{50} values. Most importantly, 3-(3-chlorophenyl)-3-hydroxypropionyl-hydroxamic acid (**6g**) exhibited high potency with IC_{50} of 0.083 ± 0.004 μM and K_i of 0.014 ± 0.003 μM, indicating that **6g** is an excellent candidate to develop novel antiulcer agent. A mixture of competitive and uncompetitive mechanism was putatively proposed to understand the inconsistency between the crystallographic and kinetic studies for the first time, which is supported by our molecular docking studies.

1. Introduction

Urease (urea amidohydrolase EC 3.5.1.5), a Ni-containing hyperactive metalloenzyme, is found in numerous bacteria, plants, fungi, algae, and some invertebrates [1,2]. It accelerates the hydrolysis of urea to ammonia and carbon dioxide by at least 10^{14} over the spontaneous reaction [3]. High concentration of ammonia arising from the reaction, as well as the accompanying pH elevation, has important negative effects in the fields of medicine and agriculture [4–6]. *Helicobacter pylori* is one of the most successful human bacterial parasites, which colonizes more than half of the human population [7]. Most infected people are asymptomatic, with moderate inflammation detectable only by biopsy and histology. However, 15–20% of them would develop severe gastroduodenal pathologies, including stomach and duodenal ulcers, adenocarcinomas and stomach lymphomas [4].

To colonize the gastroenteric tract, *H. pylori* dedicates several genes to the biosynthesis of a cytosolic urease, which buffers the pH of the bacterial immediate surroundings and creates a neutral layer around its surface. *H. pylori* urease might cause damage to the host cells through the production of ammonia, and help to recruit neutrophils and monocytes in the inflamed mucosa and to activate production of proinflammatory cytokines [8]. The essential role of urease as a virulence factor is shown by the fact that urease-defective *H. pylori* mutants cannot colonize the stomach [9]. Therefore, strategies based on urease inhibition are considered as a promising treatment for gastric and peptic ulcer caused by *H. pylori* [10]. The great medicinal potential for urease inhibitors is of high interest to researchers. Studies have been performed on this field for over 60 years, and hundreds of structures have been determined such as hydroxamic acids,

* Corresponding author. Tel.: +86 743 8563911.
** Corresponding author. School of Materials Science and Engineering, Central South University of Forestry and Technology, Changsha 410004, PR China. Tel.: +86 73 85623301.
*** Corresponding author. State Key Laboratory of Pharmaceutical Biotechnology, Nanjing University, Nanjing 210093, PR China. Tel.: +86 25 8359 2572.
E-mail addresses: xiaozhuping2005@163.com (Z.-P. Xiao), pengwanxi@163.com (W.-X. Peng), zhuhl@nju.edu.cn (H.-L. Zhu).

0223-5234/$ – see front matter © 2013 Elsevier Masson SAS. All rights reserved.
http://dx.doi.org/10.1016/j.ejmech.2013.07.047

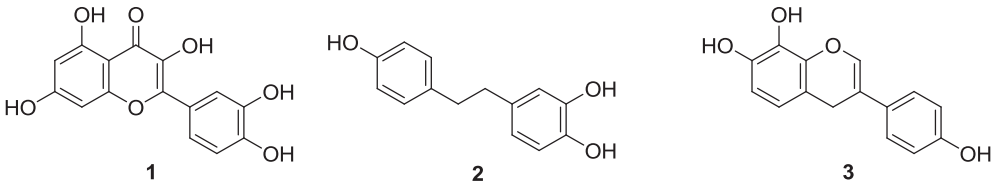

Scheme 1. Reported urease inhibitors based on flavonoids.

phosphoramidates, urea derivatives, and polyphenols [11]. Out of them, phosphoramidates are the most active but they were not marketed as drugs probably because of the rapid hydrolysis in the low pH of gastric juice [12].

Hydroxamic acids are well known to form strong complexes with a variety of transition metals, and their mechanism of inhibition involves binding to the metal ions of the active site of enzymes. Hydroxamic acids have therefore attracted much attention [13,14], and a large amount of hydroxamic acids were synthesized as inhibitors against metalloenzymes such as urease [15–17], matrix metalloproteinases [18], UDP-3-*O*-(R-3-hydroxymyristol)-*N*-acetyl-glucosamine deacetylase [19] and histone deacetylase (HDAC) [20]. The best studied urease inhibitor of hydroxamic acids is acetohydroxamic acid (AHA), which was approved as Lithostat by U.S. Food and Drug Administration in May, 1983. However, its relatively moderate inhibitory activity requires rather large doses (about 1000 mg/day for adults) [12]. Therefore, compounds with high inhibitory activity and appropriate hydrolytic stability urgently need to be discovered for the possible development of a therapy for urease mediated bacterial infections. To this end, our current efforts are focused on seeking novel urease inhibitors with good hydrolytic stability.

Very recently, we have reported flavonoids [21], deoxybenzoins [22], deoxybenzoin oximes [23], 1,2-diarylethanes [24], 3-flavenes and 2-isoflavenes [25] as urease inhibitors (Scheme 1), in which quercetin (**1**, $IC_{50} = 11.2 \pm 0.9$ μM), 4-(4-fluorophenethyl)phen-1,2-diol (**2**, $IC_{50} = 1.5 \pm 0.2$ μM) and 7,8,4-trihydroxyl-3-isoflavene (**3**, $IC_{50} = 0.85 \pm 0.06$ μM) showed significant inhibitory activity against *H. pylori* urease (Scheme 1). To the best of our knowledge, compound **3** is the first acid stable urease inhibitor with IC_{50} value being in the nanomolar range. This opened the door for discovering potent urease inhibitors with a medicinal potential based on flavonoids. By comparison of the active compound structures, a scaffold (**4**) shown as Scheme 2 would be extracted. In consideration of the high binding affinity between hydroxamic acids and transition metal ions [26], it is a clever strategy that combination of a hydroxamic acid moiety with an active compound for urease inhibitor discovering. On the other hand, hydroxamic acid moiety (**5**) could mimic a ring structure (Scheme 2). Therefore, a chimerical urease inhibitor (**6**) was designed by mimics of ring A in structure **4** with a hydroxamic acid moiety and ring C with a β-hydroxylcarbonyl moiety. In the present paper, we reported the synthesis of **6** with varying substituents on the benzene ring and the evaluation of their inhibitory activity using purified *H. pylori* urease.

2. Result and discussions

2.1. Chemistry

The *N*-hydroxy phenylacrylamide scaffold (**7**), an analog of **6**, has been employed extensively by many groups to generate potent HDAC inhibitors and has resulted in at least four clinical programs [27]. This clearly indicates that there is a great promise to get potent urease inhibitors with medicinal potential from derivatives of **6**. Based on this conception, twenty β-hydroxy-β-phenylpropionylhydroxamic acids (**6a**–**6t**) were synthesized for screen of urease inhibitors and they were all reported for the first time. Scheme 3 outlines methods where an aromatic aldehyde (**8**) was reacted with ethyl bromoacetate in THF *via* Reformatsky reaction to generate substituted ethyl 3-aryl-3-hydroxylpropionate (**9**). Subsequently, the ester (**9**) was converted to the corresponding hydroxamic acid (**6**) *via* hydroxylamine in methanolic sodium methoxide [28]. Compound **6u** was synthesized by direct hydroxyamination of ethyl 4-(*N*,*N*-dimethyl)benzoate (**10**) (Scheme 4). Compounds **6a**–**6t** were obtained in a racemic form due to a chiral center at C-3 position; fortunately, the chiral center is not included in the pharmacophore (C(O)NHOH). Therefore, the racemic mixture was not separated for urease inhibitory assays, which would not disturb us to discover inhibitors with a difference of at least one order of magnitude.

2.2. Urease inhibitory activity

We investigated substitutions to the aromatic portion in an effort to find more potent compound in comparison with our previously reported compounds (**1**, **2** and **3**). The results of the inhibition assays against *H. pylori* urease for the synthetic compounds are displayed in Table 1. In comparison with compound **6a**, introduction of a single hydroxyl or methoxy group on the phenyl ring in any position generates compounds **6b**, **6e** and **6f**, and **6j** with a less than 5-fold decrease in potency. Whereas, when a fluorine atom was introduced, the resulted compounds (**6d**, **6h** and **6m**) show a moderate increase in activities. Unexpectedly, chlorine in these positions was found to be much more potent as illustrated by compounds **6g**, **6c** and **6l**. These three compounds are the most active in their own series, showing IC_{50}s of 1.19 ± 0.08, 0.083 ± 0.004 and 3.39 ± 0.22 μM respectively. This emphasized the importance of a hydrophobic substituent in improving potency. However, replacement of the chloro substituent with a more hydrophobic substitution group, such as trifluoromethyl or benzyloxy

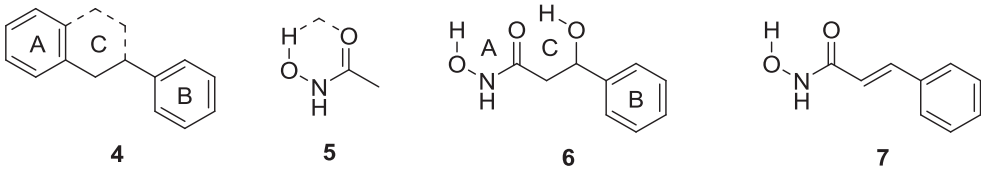

Scheme 2. Design of the hybrid hydroxamic acid (**6**).

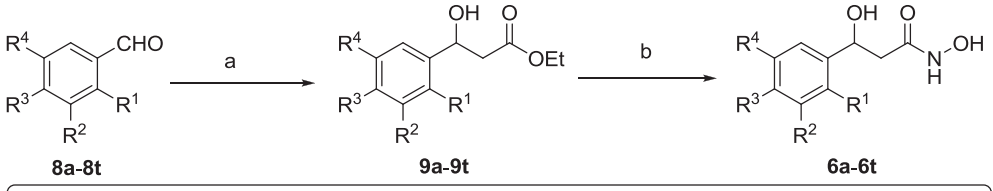

a $R^1=R^2=R^3=R^4=H$; **b** $R^2=R^3=R^4=H$, $R^1=OCH_3$; **c** $R^2=R^3=R^4=H$, $R^1=Cl$; **d** $R^2=R^3=R^4=H$, $R^1=F$; **e** $R^1=R^3=R^4=H$, $R^2=OH$; **f** $R^1=R^3=R^4=H$, $R^2=OCH_3$; **g** $R^1=R^3=R^4=H$, $R^2=Cl$; **h** $R^1=R^3=R^4=H$, $R^2=F$; **i** $R^1=R^3=R^4=H$, $R^2=CF_3$; **j** $R^1=R^2=R^4=H$, $R^3=OCH_3$; **k** $R^1=R^2=R^4=H$, $R^3=OBn$; **l** $R^1=R^2=R^4=H$, $R^3=Cl$; **m** $R^1=R^2=R^4=H$, $R^3=F$; **n** $R^1=R^2=R^4=H$, $R^3=CF_3$; **o** $R^1=R^2=R^4=H$, $R^3=NMe_2$; **p** $R^3=R^4=H$, $R^1=R^2=Cl$; **q** $R^1=R^4=H$, $R^2=R^3=Cl$; **r** $R^2=R^3=H$, $R^1=OH$, $R^4=Cl$; **s** $R^2=R^3=H$, $R^1=OCH_3$, $R^4=F$; **t** $R^3=H$, $R^1=OH$, $R^2=R^4=Cl$;

Scheme 3. Preparation of compounds **6a**–**6t**. Reagents and conditions: (a) ethyl bromoacetate, Zn, THF, reflux, 1h, 45–90%; (b) hydroxylamine hydrochloride, NaOMe, MeOH, 0 °C, 51–94%.

group, resulted in 2- to 18-fold loss of activity, illustrating that the hydrophobic area cannot comfortably accommodate these larger groups. In an effort to further understand the observed results, cLogPs of the synthesized compounds were calculated by ChemDraw Ultra 11.0 (Table 1), and the plots of IC_{50} *vs* cLogP are shown as Fig. 1. These plots clearly revealed that chloro group is the most suitable substituent for improving potency with regard to steric-hindrance and hydrophobic properties, and both a hydrophilic group and a steric-hindrance group on the phenyl ring in any position is detrimental to the activity. This is also supported by compared IC_{50}s of **6g** *vs* **6r** and **6d** *vs* **6s**.

Shifting of the fluoro or methoxy group from the C-3 (**6h** or **6f**) to the C-2 (**6d** or **6b**) position resulted in a very slight decrease in enzyme activity, while moving to the C-4 positions, as in compounds **6m** and **6j**, respectively, resulted in over 2-fold loss of activity. However, the case for chlorine is quite different. Both C-2 isomer (**6c** with IC_{50} of 1.19 ± 0.08 μM) and C-4 isomer (**6l** with IC_{50} of 3.39 ± 0.22 μM) are much less active than C-3 isomer **6g**, with 14- and 40-fold decrease in potency, respectively. Meanwhile, **6g** was the most active analog against *H. pylori* urease with activity to double digit nM numbers, showing at least a 330-fold improvement of potency compared to the commercially available urease inhibitor, AHA. This revealed that the hydrophobic 3-chloro group gets the best match to the enzyme active site among the tested compounds. Combining 3-chloro group and another substituent led to several quite active analogs (**6r**, **6t**, **6p** and **6q**) with IC_{50}s in the range of single digit μM to submicromolar. However, introducing the second substituent at C-2, C-4 and C-5 position is not beneficial to potency improvement, resulting in a 2- to 15-fold decrease in activity. In general, a higher cLogP also results in a lower IC_{50} for the multi-substituted analogs. On the basis of these findings, other possible active compounds with IC_{50} in the nanomolar range may be hit in the 3,5-disubstituted derivatives. In addition, a derivative of phenylhydroxamic acid, **6u**, with IC_{50} of 77.9 ± 7.1 μM was around 10 times less active than the corresponding the β-phenylpropionylhydroxamic acid analog (**6o**), emphasizing the importance of the ethylene link for an active compound.

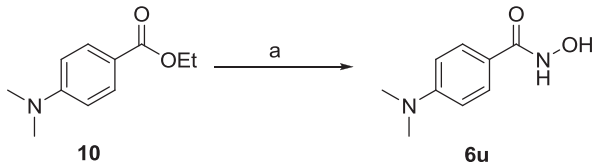

Scheme 4. Preparation of compound **6u**. Reagents and conditions: (a) hydroxylamine hydrochloride, NaOMe, MeOH, 0 °C, 2 h, 54%.

AHA and compounds with relative low IC_{50} values against cell-free urease (**6c**, **6g-i**, **6p-r** and **6t**) were selected for inhibiting urease activity in intact *H. pylori*. As shown in Table 1, the IC_{50} values of the test compounds against urease in intact cell were 3- to 9-fold higher than those for extracted urease. The higher IC_{50}s may reflect the permeability barrier of the cell surface to the compounds by *H. pylori*. Another interesting finding of this assay is that **6g** and **6p** also significantly inhibited the urease activity in intact cell. This indicates that **6g** and **6p** would be a potential urease inhibitor deserves further research.

2.3. Kinetics of urease inhibition by compounds *6g* and *6p*

Since Kobashi [29] first demonstrated in 1962 that hydroxamic acids were highly specific inhibitors of plant and bacterial original urease, many workers have extended the observations. 2001, Byung-Ha Oh et al. reported the crystal structure of *H. pylori* urease complexed with acetohydroxamic acid (AHA) [30], revealing that AHA may be a competitive inhibitor of *H. pylori* urease by binding at its active site. However, kinetic studies showed that the aliphatic

Table 1
In vitro inhibitory activity data of the synthesized compounds against *H. pylori* urease.

Entry	Compounds	cLogP	IC_{50} (μM)	
			Cell-free urease	Urease in intact cell
1	**6a**	2.142	15.6 ± 1.3	ND[a]
2	**6b**	2.061	38.5 ± 2.7	ND[a]
3	**6c**	2.855	1.19 ± 0.08	9.21 ± 0.83
4	**6d**	2.285	5.60 ± 0.34	ND[a]
5	**6e**	1.475	131 ± 9	ND[a]
6	**6f**	2.061	23.2 ± 1.7	ND[a]
7	**6g**	2.855	0.083 ± 0.004	0.36 ± 0.03
8	**6h**	2.285	3.99 ± 0.21	13.3 ± 1.2
9	**6i**	3.025	1.22 ± 0.05	6.81 ± 0.53
10	**6j**	2.061	75.1 ± 5.2	ND[a]
11	**6k**	3.829	61.5 ± 3.9	ND[a]
12	**6l**	2.855	3.39 ± 0.22	ND[a]
13	**6m**	2.285	8.01 ± 0.57	ND[a]
14	**6n**	3.025	7.89 ± 0.71	ND[a]
15	**6o**	2.307	7.13 ± 0.64	ND[a]
16	**6p**	3.448	0.23 ± 0.01	0.91 ± 0.07
17	**6q**	3.448	0.37 ± 0.02	1.42 ± 0.22
18	**6r**	2.485	1.28 ± 0.07	11.3 ± 1.9
19	**6s**	2.344	11.0 ± 0.9	ND[a]
20	**6t**	2.972	1.04 ± 0.06	8.90 ± 0.91
21	**6u**	2.307	77.9 ± 7.1	ND[a]
22	AHA		27.6 ± 2.5	110 ± 13

[a] No determination.

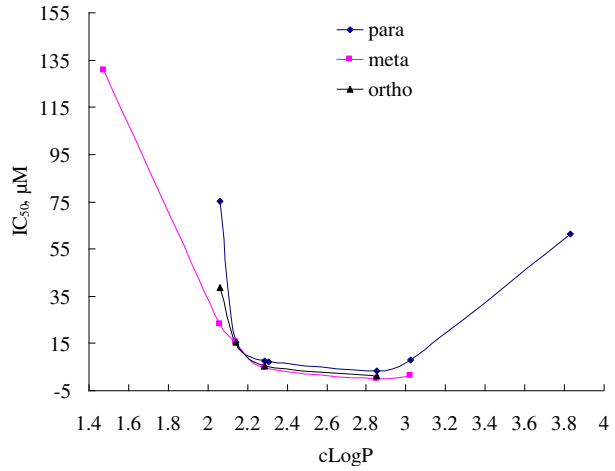

Fig. 1. The relationship of IC_{50}s and cLogPs of benzene moieties.

hydroxamic acids, including AHA, were noncompetitive inhibitors, while the aryl derivatives were of a mixed type [31]. These paradoxical results encouraged us to study the inhibition mechanism of obtained compounds. Therefore, the mechanism inhibition of urease by two selected β-hydroxy-β-phenylpropionylhydroxamic acids (**6g** and **6p**) was investigated in a kinetic inhibition with a Lineweaver–Burke plot. Double reciprocal plots of the data disclosed that **6g** and **6p** are mixed competitive inhibitors instead of the expected competitive inhibitors with respect to the substrate urea (Fig. 2A and Fig. 3A). The K_i value was calculated from a plotting of the slopes of the Lineweaver–Burk plot versus the concentration of the inhibitor (Figs. 2B and 3B) [32]. The obtained K_i values for **6g** and **6p** were 0.014 ± 0.003 and 0.045 ± 0.007 μM, demonstrating the strong affinities of them toward *H. pylori* urease.

The crystallographic studies of urease revealed that there is a flexible flap, a helix-turn-helix motif composed of residues α313–α346 [33], over the active site [30]. According to Benini et al., the highly mobile flap is in the open conformation can allow extensive access of the substrate to the active site having the best fit [34]. Urea subsequently replaces the water molecules in the native urease active site and bridges the two metal ions, which induces a change in the conformation of the flexible flap back to a closed position by rearranging the Alaα365. In the closed conformation, C–N bond of the urea molecule is broken and urea collapses into ammonia and a Ni-bound carbamate. Finally, ammonia is released from the active site, assisted by the movement of Hisα322, and the mobile flexible flap then opens. Based on this catalytic mechanism, a model was built for understand the inconsistency between the crystallographic and kinetic studies (Fig. 4). We assumed that hydroxamic acid inhibits the urease activity in a mixture of competitive and uncompetitive mechanism. According to the equilibrium of species in the enzyme reaction (Scheme 5), the enzyme kinetic equation for this mixed mechanism can be expressed as:

$$V = \frac{V_{max}[S]}{K_m\left(1+\frac{[I]}{K_i}\right)+\left(1+\frac{[I]}{K_i'}\right)[S]} \quad (1)$$

Among equation (1): $K_m = k_{-1} + k_2/k_1$, $V_{max} = k_2[E]_0$, $K_i = k_{-i}/k_i$, $K_i' = k'_{-i}/k_i'$.

Obviously, when K_i is equal to K_i', equation (1) turns into the noncompetitive kinetic equation (2):

$$V = \frac{V_{max}[S]K_i}{(K_m+[S])+(K_i+[S])} \quad (2)$$

Therefore, some hydroxamic acids are kinetically noncompetitive inhibitors, and others are acted as mixed competitive inhibitors. Although our inhibition model is quite different from the typical mixed type, they are kinetically identical. We called it as an apparent mixed competitive mechanism.

2.4. Molecular docking

In an effort to further elucidate the mixed inhibition mechanism revealed by the kinetic study and to confirm our assumed inhibition model (Scheme 5), we performed molecular docking studies. The most active compound (**6g**) was selected to dock with *H. pylori* urease (entry 1E9Y in the Protein Data Bank) by the AutoDock program. As above mentioned, **6g** was formed as a raceme. Thus, docking studies were performed on both possible configurations (R and S) to evaluate if one or both enantiomers could be actually interacting with the biological target. The binding results of R-**6g** and S-**6g** are shown as both enzyme surface (Fig. 5A and B) and cartoon modes (Figure 6A and B, 7A and 7B), respectively. On one hand, the binding models revealed that R-**6g** and S-**6g** nearly fill equivalent spaces, suggesting that they should display a similar potency against *H. pylori* urease. On the other hand, the models disclosed that both R-**6g** and S-**6g** showed two best possible binding modes, respectively. One is well filled in the active pocket

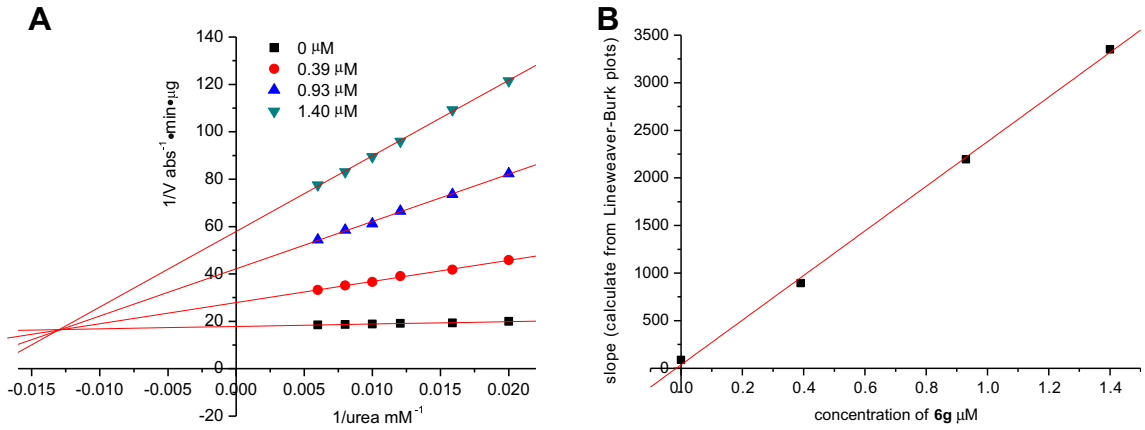

Fig. 2. (A) Lineweaver–Burk plot for the inhibition of urease by **6g**. Data were obtained in three different experiments with triplicates. (B) The plots of the slopes from the Lineweaver–Burk lines *vs.* different concentrations of inhibitor.

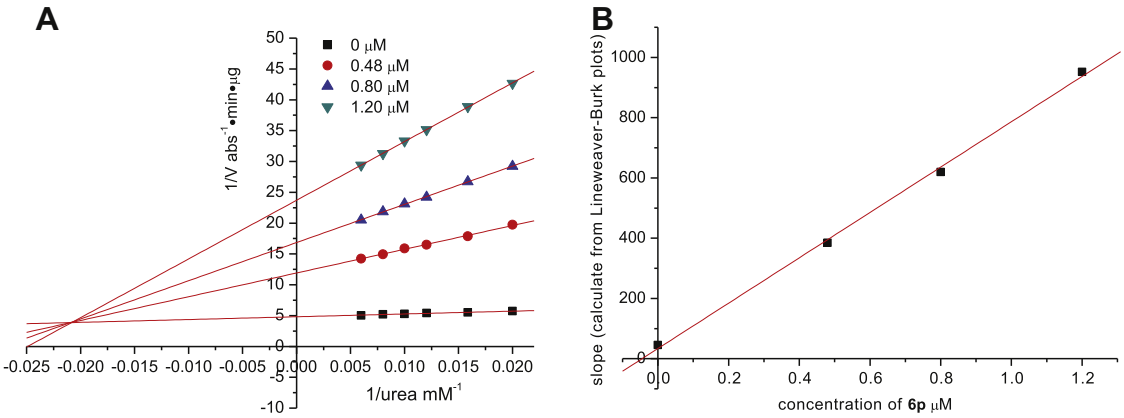

Fig. 3. (A) Lineweaver–Burk plot for the inhibition of urease by **6p**. Data were obtained in three different experiments with triplicates. (B) The plots of the slopes from the Lineweaver–Burk lines *vs*. different concentrations of inhibitor.

(defined as mode A, Figs. 5A, 6A and B) and the other is tightly anchored at beside the entrance of the active site (defined as mode B, Figs. 5B, 7A and B).

In the three-dimensional models (Figs. 6A and 7A) of the S-**6g**, it is important to note that the acylhydroxamic acid moiety (C(O)NHOH) is of primary importance for its interactions network. In mode A (Fig. 6A), S-**6g** binds the active site in an anion form (C(O)NHO^-), in which the oxygen ion bridges the two nickel ions with metal–ligand distance of 2.060 and 2.175 Å, respectively. The carbonyl oxygen shows a hydrogen bonding interaction with the NH_2 group of His221 at a distance of 3.293 Å and a metal–ligand interaction with a distance of 3.205 Å, NH group of S-**6g** was found to strongly hydrogen bond with the carbonyl group of Ala365 at a distance of 2.354 Å. The same NH group interacted with the both oxygens of Asp362 at distances of 2.104 and 3.135 Å, respectively. In addition to the tightly bound acylhydroxamic acid moiety, S-**6g** is further anchored to the active site by a strong hydrogen bond (2.279 Å) between its β-hydroxyl group and Asn168. The benzene ring is sandwiched in between Cys321, Ala365 and Met366 through a S–H·π hydrogen bonding interaction and hydrophobic interactions within a distance of 3.5 Å. Fig. 6B depicts the 3D model of the interaction between R-**6g** and the target, which revealed that the interaction network is nearly consistent with that of S-**6g**. This binding mode undoubtedly confirms the characteristic of kinetically competitive inhibition of **6g**.

In mode B, S-**6g** and R-**6g** were docked with *H. pylori* urease in a neutral molecule form (Fig. 7A and B). By comparison with mode A, S-**6g** or R-**6g** is located under the flexible flap (residues α313–α346) over the active site, with the benzene ring filling in the gap between Cys321, Ala365 and Met366 and with the acylhydroxamic acid moiety forming an extensive hydrogen bonding network. S-**6g** using the oxygen of hydroxamic acid moiety (NHOH) as an acceptor receives a hydrogen bonding interaction (3.590 Å) from Gly367 and as a donor forms two hydrogen bond with Gln364 (3.728 Å) and Ala365 (2.973 Å). While R-**6g** using the same oxygen as an acceptor receives two hydrogen bonding interactions (3.484 and 3.555 Å) from Gly367 and Ala365, and as a donor forms only one hydrogen bond with Met366 (2.012 Å). A strong hydrogen bonding interaction with a distance of 2.443 Å was observed between the carbonyl group of S-**6g** and the back bone NH of Met366. As for R-**6g**, this hydrogen bond is lightly weak (2.525 Å). β-Hydroxyl group of S-**6g** or R-**6g** tightly anchor the flexible flap of the enzyme by two hydrogen bonding interactions built by Met317 and Val320. The movable flap is further fixed by the S–H·π contacts occurred

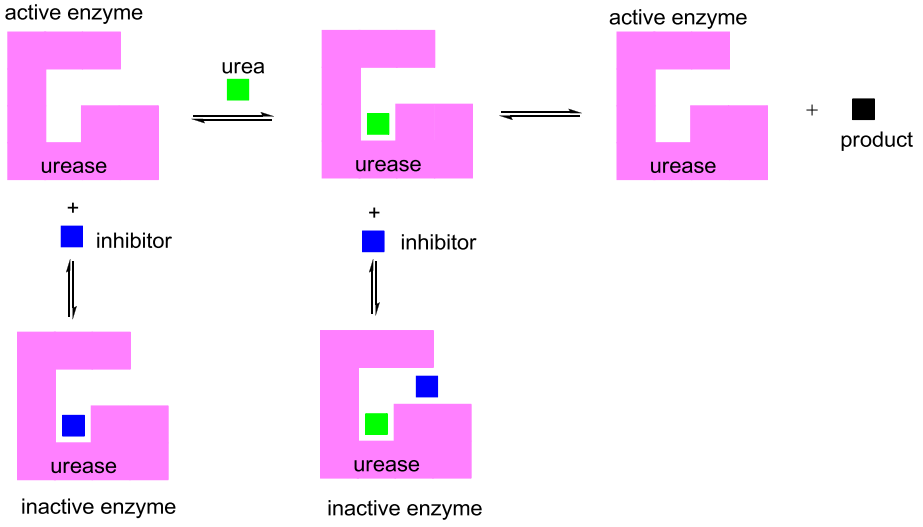

Fig. 4. The assumed mechanism mode mixed by competitive and uncompetitive inhibition.

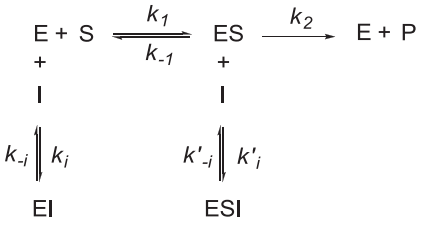

Scheme 5. The equilibrium of species in the enzyme reaction for the assumed inhibition mechanism.

between Cys321 and the benzene ring of S-**6g** or R-**6g**, while the benzene ring is stabled by the hydrophobic interactions from Met366 and Ala365. S-**6g** or R-**6g** in the current pose, like a support frame, blocks the flap to move. According to Benini et al., the flap must be in a closed conformation, before C–N bond of the urea molecule was broken and urea collapsed into ammonia and a Ni-bound carbamate. Therefore, urease will not complete the catalytic hydrolysis of urea without the movement of this flap, leading to an inactive enzyme. This inactive urease complex will be formed only after a urea molecule is in the active site, which provides a rational explanation for the kinetically uncompetitive inhibition characteristic of hydroxamic acids.

It is well known that hydroxamic acid is a weak acid (pKa of 8 for AHA). Therefore, a typical hydroxamic acid is presents as an equilibrium mixture of molecule and anion forms under physiological condition. Our molecular docking modes disclosed that both molecule and anion of hydroxamic acid are all potent inhibitors of *H. pylori* urease, but show different actions of kinetics. This makes hydroxamic acid inhibits *H. pylori* urease in an apparent mixed mechanism.

3. Conclusion

A total of twenty hybrids of flavonoid scaffold and hydroxamic acid, β-hydroxy-β-phenyl-propionylhydroxamic acids, were synthesized, tested for urease activity, and docked to *H. pylori* urease. Many compounds exhibit micromolar to low micromolar IC_{50} values in the *in vitro H. pylori* urease inhibition assay. Kinetic studies of two representative derivatives (**6g** and **6p**) suggested a mixed type of inhibition mechanism. While, the molecular docking of the most active compound, **6g** (IC_{50} = 0.083 ± 0.004 μM), further revealed that the two possible enantiomers of **6g** may display a similar potency against *H. pylori* urease and inhibit urease with a mixture of competitive and uncompetitive mechanism. The excellent potency of **6g** and **6p** against *H. pylori* urease suggests that they deserve to be further researched as a good candidate to treat gastritis and gastric ulcer. More detailed studies of the pharmacological profiles of these promising compounds are underway in our lab. Meanwhile, using **6g** and **6p** as leads, continued efforts are also underway to search more potent urease inhibitors.

4. Experimental section

4.1. Biology materials

Protease inhibitors (Complete mini EDTA-free) were purchased from Roche Diagnostics GmbH (Mannheim, Germany) and Brucella broth was from Becton–Dickinson (Cockeysville, MD). Horse serum was from Hyclone (Utah, American).

4.2. Bacteria

H. pylori (ATCC 43504; American Type Culture Collection, Manassas, VA) was grown in Brucella broth supplemented with 10% heat-inactivated horse serum for 24 h at 37 °C under microaerobic conditions (5% O_2, 10% CO_2, and 85% N_2), as our previously described [21–25].

4.3. Preparation of H. pylori urease

For urease inhibition assays, 50 mL broth cultures (2.0×10^8 CFU/mL) were centrifuged (5000 g, 4 °C) to collect the bacteria, and after washing twice with phosphate-buffered saline (pH 7.4), the *H. pylori* precipitation was stored at −80 °C. *H. pylori* was returned to room temperature, and after addition of 3 mL of distilled water and protease inhibitors, sonication was performed for 60 s. Following centrifugation (15,000× *g*, 4 °C), the supernatant was desalted through Sephadex G-25 column (PD-10 columns, Amersham Pharmacia Biotech, Uppsala, Sweden). The resultant crude urease solution was added to an equal volume of glycerol and stored at 4 °C until use in the experiment.

4.4. Measurement of urease inhibitory activity

The assay mixture, containing 25 μL (10U) of *H. pylori* urease which was replaced by 25 μL of cell suspension (4.0×10^7 CFU/mL) for the urease assay of intact cells and 25 μL of the test compound, was pre-incubated for 1.5 h at room temperature in a 96-well assay plate. Urease activity was determined by measuring ammonia

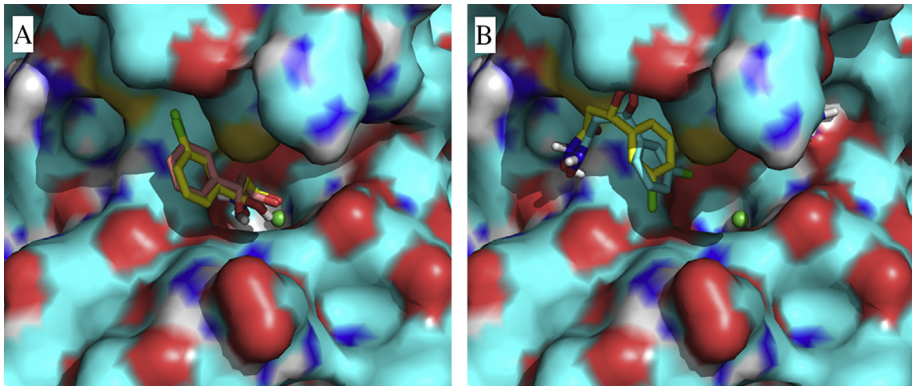

Fig. 5. Binding modes of compound **6g** with *H. pylori* urease. The enzyme is shown as surface; while **6g** is shown as sticks. (A) **6g** docked as molecule forms (R-**6g**, yellow; S-**6g**, salmon); (B) **6g** docked as anion forms (R-**6g**, cyan; S-**6g**, yellow). (For interpretation of the references to colour in this figure legend, the reader is referred to the web version of this article.)

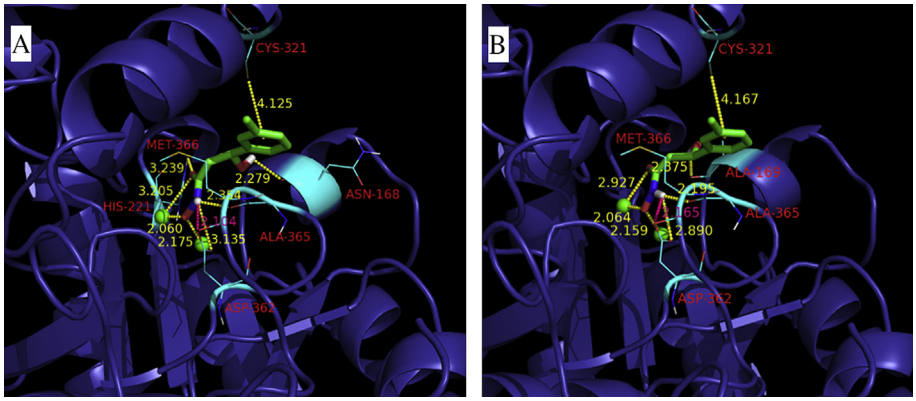

Fig. 6. Binding modes of compound **6g** with *H. pylori* urease. The enzyme is shown as cartoon; while **6g** is shown as sticks. (A) S-**6g** docked as anion form; (B) R-**6g** docked as anion form.

production using the indophenol method as described by Weatherburn [35].

4.5. Kinetic study

Lineweaver–Burk plots of 1/absorbance versus 1/urea were used to determine the type of enzyme inhibition. Urease inhibition was measured by varying the concentration of urea in the presence of different concentrations of **6g** or **6p**. Inhibitory constants (K_i) were determined as the intersection on the *X*-axis of the plots of the slopes *vs.* different concentrations of inhibitor, in which the slopes obtained from the Lineweaver–Burk lines. All experiments were conducted in triplicate.

4.6. Protocol of docking study

The automated docking studies were carried out using AutoDock version 4.2. First, AutoGrid component of the program precalculates a three-dimensional grid of interaction energies based on the macromolecular target using the AMBER force field. The cubic grid box of 62 Å size (x, y, z) with a spacing of 0.375 Å for mode A (85 Å for mode B) and grid maps were created representing the catalytic active target site region where the native ligand was embedded. Then automated docking studies were carried out to evaluate the binding free energy of the inhibitor within the macromolecules. The GALS search algorithm (genetic algorithm with local search) was chosen to search for the best conformers. The parameters were set using the software ADT (AutoDockTools package, version 1.5.4) on PC which is associated with AutoDock 4.2. Default settings were used with an initial population of 50 randomly placed individuals, a maximum number of 2.5×10^6 energy evaluations, and a maximum number of 2.7×10^4 generations. A mutation rate of 0.02 and a crossover rate of 0.8 were chosen. Results differing by less than 0.5 Å in positional root-mean-square deviation (RMSD) were clustered together and the results of the most favorable free energy of binding were selected as the resultant complex structures.

4.7. Chemistry

All chemicals (reagent grade) used were purchased from Aldrich (U.S.A) and Sinopharm Chemical Reagent Co., Ltd (China). Melting points (uncorrected) were determined on an XT4 MP apparatus (Taike Corp., Beijing, China). EI mass spectra were obtained on a Waters GCT mass spectrometer, and ^{1}H NMR spectra were recorded on a Bruker AV-300 spectrometer at 25 °C with TMS and solvent signals allotted as internal standards. Chemical shifts were reported in ppm (δ). Elemental analyses were performed on a CHN–O-Rapid instrument and were within ±0.4% of the theoretical values.

4.7.1. General procedure for the preparation of compounds ***9a–9t***

Zinc powder is treated with 2% HCl to give activated zinc. After the suspension of activated zinc (10 mmol) in dry THF (8 mL) is heated to reflux, the heating is stopped, and a solution of ethyl

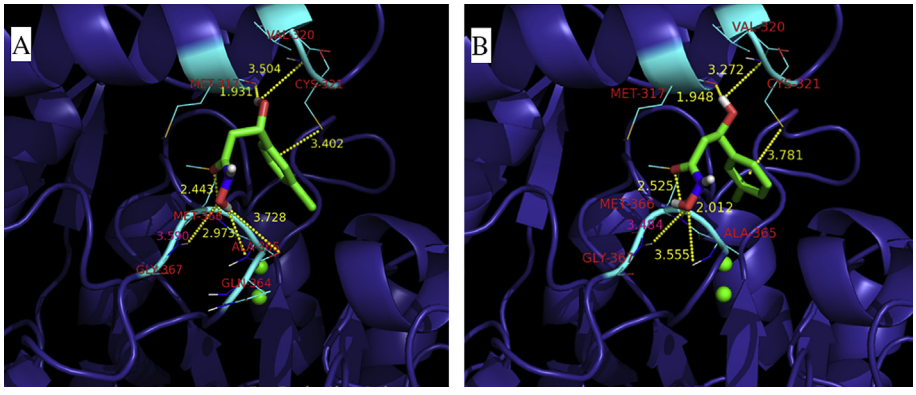

Fig. 7. Binding modes of compound **6g** with *H. pylori* urease. The enzyme is shown as cartoon; while **6g** is shown as sticks. (A) S-**6g** docked as molecule form; (B) R-**6g** docked as molecule form.

bromoacetate (6 mmol) and appropriate substituted benzaldehyde (**8**, 5 mmol) in dry THF (5 mL) is added within 30 min. After being heated to reflux for 0.5–3 h, the mixture is cooled and magnetically stirred for 15 min with saturated NH_4Cl (20 mL). The aqueous phase is extracted with AcOEt (2 × 50 mL) and the combined organic phases are washed with a 5% $NaHCO_3$ solution (2 × 20 mL). After drying over $MgSO_4$, concentration under reduced pressure furnishes a residue, which is purified over a silica gel column eluting with AcOEt-petroleum ether to yield an ester **9**.

*4.7.2. General procedure for the preparation of compounds **6a**–**6u***

To a stirred solution of sodium methoxide (10 mmol) and 6 mmol of hydroxylamine hydrochloride at 0 °C is added an ester (**9** or **10**, 3 mmol). The reaction is monitored by TLC, and upon completion the reaction mixture is brought to pH 7–8 with 1 M hydrochloric acid. The resulted mixture is extracted thrice with AcOEt, and the combined organic layer washes with brine. After drying over $MgSO_4$, removement of the solvent under reduced pressure give a slight yellow oil. Compound **6** is obtained after purification with column chromatography on silica gel, eluting with AcOEt-petroleum ether.

*4.7.2.1. 3-Hydroxy-3-phenylpropionylhydroxamic acid (**6a**).* White powder, 52%, mp 156–158 °C, ^{1}H NMR (DMSO-d_6): 2.26–2.41 (m, 2H); 3.7–4.5 (bs, 1H); 5.06 (dd, J = 8.0 Hz, J = 5.1 Hz, 1H); 7.48–7.56 (m, 5H); 7.94 (s, 1H); 10.36 (bs, 1H); EIMS m/z 181 (M^+). Anal. Calcd for $C_9H_{11}NO_3$: C, 59.66; H, 6.12; N, 7.73; Found: C, 59.63; H, 6.12; N, 7.74.

*4.7.2.2. 3-Hydroxy-3-(2-methoxyphenyl)propionylhydroxamic acid (**6b**).* White powder, 54%, mp 124–126 °C, ^{1}H NMR ($CDCl_3$): 2.25 (dd, J = 13.5 Hz, J = 9.0 Hz, 1H); 2.48 (dd, J = 13.4 Hz, J = 2.5 Hz, 1H); 4.43–4.50 (m, 1H); 5.17 (d, J = 6.5 Hz, 1H); 7.14 (t, J = 7.5 Hz, 1H); 7.27 (t, J = 7.7 Hz, 2H); 7.48 (d, J = 7.1 Hz, 1H); 7.85 (s, 1H); 10.38 (bs, 1H); ^{13}C NMR (DMSO-d_6): 41.7, 55.5, 63.7, 115.6, 124.8, 128.2, 129.3, 132.5, 158.2, 167.0; EIMS m/z 211 (M^+). Anal. Calcd for $C_{10}H_{13}NO_4$: C, 56.86; H, 6.20; N, 6.63; Found: C, 56.92; H, 6.19; N, 6.62.

*4.7.2.3. 3-(2-Chlorophenyl)-3-hydroxypropionylhydroxamic acid (**6c**).* White powder, 67%, mp 181–183 °C, ^{1}H NMR ($CDCl_3$): 2.27 (dd, J = 14.1 Hz, J = 9.4 Hz, 1H); 2.51 (dd, J = 14.4 Hz, J = 2.7 Hz, 1H); 4.43–4.52 (m, 1H); 5.38 (d, J = 6.9 Hz, 1H); 7.21 (t, J = 7.5 Hz, 1H); 7.30 (t, J = 7.7 Hz, 2H); 7.50 (d, J = 7.1 Hz, 1H); 7.81 (s, 1H); 10.40 (bs, 1H); EIMS m/z 215 (M^+). Anal. Calcd for $C_9H_{10}ClNO_3$: C, 50.13; H, 4.67; Cl, 16.44; N, 6.50; Found: C, 50.18; H, 4.66; Cl, 16.42; N, 6.51.

*4.7.2.4. 3-(2-Fluorophenyl)-3-hydroxypropionylhydroxamic acid (**6d**).* White powder, 92%, mp 138–140 °C, ^{1}H NMR ($CDCl_3$): 2.26 (dd, J = 14.0 Hz, J = 9.2 Hz, 1H); 2.47 (dd, J = 14.2 Hz, J = 2.8 Hz, 1H); 4.41–4.49 (m, 1H); 5.23 (d, J = 7.0 Hz, 1H); 7.22 (t, J = 7.4 Hz, 1H); 7.33 (t, J = 7.6 Hz, 2H); 7.48 (t, J = 7.5 Hz, 1H); 7.85 (s, 1H); 10.36 (bs, 1H); ^{13}C NMR (DMSO-d_6): 43.0, 69.3, 125.0, 126.1, 127.3, 130.5, 133.3, 148.4, 167.0; EIMS m/z 199 (M^+). Anal. Calcd for $C_9H_{10}FNO_3$: C, 54.27; H, 5.06; F, 9.54; N, 7.03; Found: C, 54.19; H, 5.06; F, 9.56; N, 7.05.

*4.7.2.5. 3-Hydroxy-3-(3-hydroxyphenyl)propionylhydroxamic acid (**6e**).* White powder, 70%, mp 163–165 °C, ^{1}H NMR (DMSO-d_6): 2.27–2.35 (m, 2H); 4.10–5.10 (m, 1H); 4.88 (dd, J = 8.0 Hz, J = 5.1 Hz, 1H); 6.59 (dd, J = 7.3 Hz, J = 2.0 Hz, 1H); 6.73 (d, J = 7.7 Hz, 1H); 6.77 (s, 1H); 7.02 (t, J = 7.9 Hz, 1H); 7.66 (s, 1H); 10.25 (bs, 1H); EIMS m/z 197 (M^+). Anal. Calcd for $C_9H_{11}NO_4$: C, 54.82; H, 5.62; N, 7.10; Found: C, 54.77; H, 5.61; N, 7.12.

*4.7.2.6. 3-Hydroxy-3-(3-methoxyphenyl)propionylhydroxamic acid (**6f**).* White powder, 94%, mp 150–151 °C, ^{1}H NMR (DMSO-d_6): 2.07 (dd, J = 13.9 Hz, J = 9.6 Hz, 1H); 2.27 (dd, J = 14.1 Hz, J = 2.9 Hz, 1H); 3.78 (s, 1H); 5.15 (d, J = 4.6 Hz, 1H); 5.22–5.29 (m, 1H); 6.90–6.96 (m, 2H); 7.21 (t, J = 6.9 Hz, 1H); 7.41 (d, J = 7.3 Hz, 1H); 8.71 (s, 1H); 10.31 (s, 1H); ^{13}C NMR (DMSO-d_6): 41.4, 55.8, 64.0, 110.9, 120.7, 126.5, 128.3, 133.8, 155.8, 167.8; EIMS m/z 211 (M^+). Anal. Calcd for $C_{10}H_{13}NO_4$: C, 56.86; H, 6.20; N, 6.63; Found: C, 56.91; H, 6.20; N, 6.61.

*4.7.2.7. 3-(3-Chlorophenyl)-3-hydroxypropionylhydroxamic acid (**6g**).* White powder, 76%, mp 125–127 °C, ^{1}H NMR (DMSO-d_6): 2.26–2.40 (m, 2H); 4.80–6.00 (bs, 1H); 4.97 (dd, J = 8.0 Hz, J = 5.1 Hz, 1H); 7.12–7.24 (m, 3H); 7.33 (s, 1H); 7.81 (s, 1H); 10.32 (bs, 1H); ^{13}C NMR (DMSO-d_6): 43.0, 69.3, 125.0, 126.1, 127.3, 130.5, 133.3, 148.4, 167.0; EIMS m/z 215 (M^+). Anal. Calcd for $C_9H_{10}ClNO_3$: C, 50.13; H, 4.67; Cl, 16.44; N, 6.50; Found: C, 50.18; H, 4.66; Cl, 16.42; N, 6.50.

*4.7.2.8. 3-(3-Fluorophenyl)-3-hydroxypropionylhydroxamic acid (**6h**).* White powder, 65%, mp 115–117 °C, ^{1}H NMR (DMSO-d_6): 2.20–2.33 (m, 2H); 4.92–4.99 (m, 1H); 5.52 (d, J = 4.6 Hz, 1H); 7.05 (t, J = 9.0 Hz, 1H); 7.14 (t, J = 7.3 Hz, 1H); 7.16 (d, J = 12.2 Hz, 1H); 7.35 (dd, J = 13.0 Hz, J = 7.5 Hz, 1H); 8.74 (s, 1H); 10.34 (s, 1H); EIMS m/z 199 (M^+). Anal. Calcd for $C_9H_{10}FNO_3$: C, 54.27; H, 5.06; F, 9.54; N, 7.03; O, 24.10; Found: C, 54.34; H, 5.05; F, 9.52; N, 7.02.

*4.7.2.9. 3-Hydroxy-3-(3-trifluoromethylphenyl)propionylhydroxamic acid (**6i**).* White powder, 62%, mp 126–128 °C, ^{1}H NMR (DMSO-d_6): 2.30–2.38 (m, 2H); 5.01–5.07 (m, 1H); 5.62 (d, J = 4.6 Hz, 1H); 7.52–7.64 (m, 3H); 7.68 (s, 1H); 8.75 (s, 1H); 10.36 (s, 1H); ^{13}C NMR (DMSO-d_6): 43.0, 69.2, 122.6, 122.64, 124.1, 124.2, 129.6, 130.5, 147.2, 166.9; EIMS m/z 249 (M^+). Anal. Calcd for $C_{10}H_{10}F_3NO_3$: C, 48.20; H, 4.04; F, 22.87; N, 5.62; Found: C, 48.12; H, 4.05; F, 22.89; N, 5.61.

*4.7.2.10. 3-Hydroxy-3-(4-methoxyphenyl)propionylhydroxamic acid (**6j**).* White powder, 73%, mp 113–114 °C, ^{1}H NMR (DMSO-d_6): 2.19–2.35 (m, 2H); 3.73 (s, 1H); 4.85–4.92 (m, 1H); 5.25 (d, J = 4.4 Hz, 1H); 6.88 (d, J = 8.6 Hz, 2H); 7.24 (d, J = 8.8 Hz, 2H); 8.70 (s, 1H); 10.32 (s, 1H); ^{13}C NMR (DMSO-d_6): 43.3, 55.5, 69.5, 113.9, 127.4, 137.7, 158.7, 167.4; EIMS m/z 211 (M^+). Anal. Calcd for $C_{10}H_{13}NO_4$: C, 56.86; H, 6.20; N, 6.63; Found: C, 56.78; H, 6.21; N, 6.64.

*4.7.2.11. 3-(4-Benzyloxyphenyl)-3-hydroxypropionylhydroxamic acid (**6k**).* White powder, 60%, mp 124–129 °C, ^{1}H NMR (DMSO-d_6): 2.21–2.35 (m, 2H); 4.18 (s, 2H); 4.83–4.91 (m, 1H); 5.32 (d, J = 4.6 Hz, 1H); 6.86 (d, J = 8.7 Hz, 2H); 7.27 (d, J = 8.8 Hz, 2H); 7.47–7.55 (m, 5H); 8.65 (s, 1H); 10.35 (s, 1H); EIMS m/z 287 (M^+). Anal. Calcd for $C_{16}H_{17}NO_4$: C, 66.89; H, 5.96; N, 4.88; Found: C, 66.96; H, 5.95; N, 4.87.

*4.7.2.12. 3-(4-Chlorophenyl)-3-hydroxypropionylhydroxamic acid (**6l**).* White powder, 62%, mp 159–162 °C, ^{1}H NMR (DMSO-d_6): 2.20–2.36 (m, 2H); 4.90–5.00 (m, 1H); 5.47 (d, J = 4.6 Hz, 1H); 7.32–7.37 (m, 4H); 8.73 (bs, 1H); 10.34 (bs, 1H); ^{13}C NMR (DMSO-d_6): 43.1, 69.2, 128.1, 128.5, 131.8, 144.8, 167.0; EIMS m/z 215 (M^+). Anal. Calcd for $C_9H_{10}ClNO_3$: C, 50.13; H, 4.67; Cl, 16.44; N, 6.50; Found: C, 50.18; H, 4.67; Cl, 16.42; N, 6.49.

*4.7.2.13. 3-(4-Fluorophenyl)-3-hydroxypropionylhydroxamic acid (**6m**).* White powder, 53%, mp 130–132 °C, ^{1}H NMR (DMSO-d_6): 2.19–2.35 (m, 2H); 4.91–4.97 (m, 1H); 5.42 (d, J = 4.6 Hz, 1H); 7.13 (d, J = 8.8 Hz, 2H); 7.35 (dd, J = 8.7 Hz, J = 5.6 Hz, 2H); 8.72 (s, 1H); 10.33 (s, 1H); EIMS m/z 199 (M^+). Anal. Calcd for $C_9H_{10}FNO_3$: C, 54.27; H, 5.06; F, 9.54; N, 7.03; Found: C, 54.20; H, 5.01; F, 9.56; N, 7.02.

*4.7.2.14. 3-Hydroxy-3-(4-trifluorophenyl)propionylhydroxamic acid (**6n**).* White powder, 68%, mp 158–160 °C, ^{1}H NMR (DMSO-d_6): 2.40–2.46 (m, 2H); 4.00–4.80 (bs, 1H); 5.11–5.16 (m, 1H); 7.52–7.60 (m, 4H); 7.75 (s, 1H); 10.39 (s, 1H); EIMS *m/z* 249 (M^+). Anal. Calcd for $C_{10}H_{10}F_3NO_3$: C, 48.20; H, 4.04; F, 22.87; N, 5.62; Found: C, 48.28; H, 4.04; F, 22.85; N, 5.61.

*4.7.2.15. 3-Hydroxy-3-[(4-N,N-dimethylamino)phenyl]propionylhydroxamic acid (**6o**).* White powder, 65%, mp 152–154 °C, ^{1}H NMR (DMSO-d_6): 2.23–2.38 (m, 2H); 3.68 (s, 6H); 4.92–4.98 (m, 1H); 5.43 (d, J = 4.6 Hz, 1H); 6.86 (d, J = 8.7 Hz, 2H); 7.23 (d, J = 8.6 Hz, 2H); 7.80 (s, 1H); 10.34 (s, 1H); EIMS *m/z* 224 (M^+). Anal. Calcd for $C_{11}H_{16}N_2O_3$: C, 58.91; H, 7.19; N, 12.49; Found: C, 58.84; H, 7.20; N, 12.52.

*4.7.2.16. 3-(2,3-Dichlorophenyl)-3-hydroxypropionylhydroxamic acid (**6p**).* White powder, 80%, mp 112–113 °C, ^{1}H NMR (DMSO-d_6): 2.18–2.26 (m, 2H); 4.88–4.94 (m, 1H); 5.42 (d, J = 4.6 Hz, 1H); 6.81 (d, J = 8.7 Hz, 1H); 7.03 (t, J = 8.5 Hz, 1H); 7.21 (d, J = 8.8 Hz, 1H); 7.82 (s, 1H); 10.31 (s, 1H); ^{13}C NMR (DMSO-d_6): 42.8, 68.8, 126.7, 128.3, 129.8, 130.8, 131.2, 146.9, 166.8; EIMS *m/z* 249 (M^+). Anal. Calcd for $C_9H_9Cl_2NO_3$: C, 43.22; H, 3.63; Cl, 28.35; N, 5.60; Found: C, 43.28; H, 3.63; Cl, 28.33; N, 5.59.

*4.7.2.17. 3-(3,4-Dichlorophenyl)-3-hydroxypropionylhydroxamic acid (**6q**).* White powder, 82%, mp 135–137 °C, ^{1}H NMR (DMSO-d_6): 2.25–2.41 (m, 2H); 4.96–5.04 (m, 1H); 5.46 (d, J = 4.4 Hz, 1H); 6.83 (d, J = 8.8 Hz, 1H); 7.17 (d, J = 8.6 Hz, 1H); 7.31 (s, 1H); 7.76 (s, 1H); 10.36 (s, 1H); EIMS *m/z* 249 (M^+). Anal. Calcd for $C_9H_9Cl_2NO_3$: C, 43.22; H, 3.63; Cl, 28.35; N, 5.60; Found: C, 43.15; H, 3.64; Cl, 28.37; N, 5.61.

*4.7.2.18. 3-(5-Chloro-2-hydroxyphenyl)-3-hydroxypropionylhydroxamic acid (**6r**).* White powder, 77%, mp 92–93 °C, ^{1}H NMR (DMSO-d_6): 2.31 (dd, J = 14.6 Hz, J = 8.8 Hz, 1H); 2.52 (dd, J = 14.6 Hz, J = 3.8 Hz, 1H); 3.50–4.50 (bs, 1H); 5.23 (dd, J = 8.8 Hz, J = 3.7 Hz, 1H); 6.76 (d, J = 8.6 Hz, 1H); 6.99 (dd, J = 8.6 Hz, J = 2.7 Hz, 2H); 7.31 (d, J = 2.6 Hz, 1H); 7.89 (s, 1H); 9.38 (bs, 1H); 10.38 (bs, 1H); ^{13}C NMR (DMSO-d_6): 40.8, 64.3, 116.9, 122.9, 126.4, 127.5, 134.4, 152.8, 167.6; EIMS *m/z* 231 (M^+). Anal. Calcd for $C_9H_{10}ClNO_4$: C, 46.67; H, 4.35; Cl, 15.31; N, 6.05; Found: C, 46.61; H, 4.35; Cl, 15.32; N, 6.06.

*4.7.2.19. 3-(5-Fluoro-2-methoxyphenyl)-3-hydroxypropionylhydroxamic acid (**6s**).* White powder, 87%, mp 127–129 °C, ^{1}H NMR (DMSO-d_6): 2.30–2.50 (m, 2H); 3.78 (s, 3H); 4.20–5.10 (bs, 1H); 5.24 (t, J = 6.4 Hz, 1H); 6.58 (dd, J = 9.0 Hz, J = 2.2 Hz, 1H); 6.69 (d, J = 8.6 Hz, 1H); 7.41 (t, J = 8.7 Hz, 1H); 7.83 (s, 1H); 10.38 (bs, 1H); ^{13}C NMR (DMSO-d_6): 41.8, 56.0, 63.5, 101.7, 110.6, 124.2, 128.8, 158.8, 160.1, 167.1; EIMS *m/z* 229 (M^+). Anal. Calcd for $C_{10}H_{12}FNO_4$: C, 52.40; H, 5.28; F, 8.29; N, 6.11; Found: C, 52.48; H, 5.27; F, 8.27; N, 6.10.

*4.7.2.20. 3-(3,5-Dichloro-2-hydroxyphenyl)-3-hydroxypropionyl hydroxamic acid (**6t**).* White powder, 51%, mp 129–131 °C, ^{1}H NMR (DMSO-d_6): 2.10–2.30 (m, 1H); 2.30–2.48 (m, 1H); 5.21 (bs, 1H); 7.26 (s, 1H); 7.35 (s, 1H); 8.8 (bs, 1H); 10.35 (bs, 1H); EIMS *m/z* 265 (M^+). Anal. Calcd for $C_9H_9Cl_2NO_4$: C, 40.63; H, 3.41; Cl, 26.65; N, 5.26; Found: C, 40.55; H, 3.41; Cl, 26.68; N, 5.27.

*4.7.2.21. 4-Dimethylaminophenylhydroxamic acid (**6u**).* White powder, 54%, mp 148–150 °C, ^{1}H NMR (DMSO-d_6): 2.93 (s, 6H); 2.30–2.48 (m, 1H); 6.70 (d, J = 8.8 Hz, 2H); 7.39 (d, J = 8.8 Hz, 2H); 7.96 (s, 1H); 10.64 (s, 1H); EIMS *m/z* 180 (M^+). Anal. Calcd for $C_9H_{12}N_2O_2$: C, 59.99; H, 6.71; N, 15.55; Found: C, 59.90; H, 6.71; N, 15.57.

Acknowledgment

The work was financed by grants from National Natural Science Foundation (grant Nos. 81273382) of China, by a Project supported by Hunan Provincial Natural Science Foundation of China (grant No. 11JJ3113 and 13JJ2030), by a grant from National Natural Science Foundation (Youth Science Funds, No. 31100421) of China and by aid program for Science and Technology Innovative Research Team (Chemicals of Forestry Resources and Development of Forest Products) in Higher Educational Institutions of Hunan Province.

Appendix A. Supplementary data

Supplementary data related to this article can be found at http://dx.doi.org/10.1016/j.ejmech.2013.07.047.

References

[1] B. Krajewska, J. Mol. Catal. B Enzym. 59 (2009) 9–21.
[2] B. Krajewska, R. van Eldik, M. Brindell, J. Biol. Inorg. Chem. 17 (2012) 1123–1134.
[3] Zaheer-ul-Haq, M.A. Lodhi, S.A. Nawaz, S. Iqbal, K.M. Khan, B.M. Rode, Atta-ur-Rahman, M.I. Choudhary, Bioorgan. Med. Chem. 16 (2008) 3456–3461.
[4] C. Montecucco, R. Rappuoli, Nat. Rev. Mol. Cell Biol. 2 (2001) 457–466.
[5] Z.L. You, D.M. Xian, M. Zhang, X.S. Cheng, X.F. Li, Bioorgan. Med. Chem. 20 (2012) 4889–4894.
[6] S. Firdous, N.H. Ansari, I. Fatima, A. Malik, N. Afza, L. Iqbal, M. Lateef, Arch. Pharm. Res. 35 (2012) 1133–1137.
[7] J. Parsonnet, Aliment. Pharmacol. Ther. 9 (Suppl. 2) (1995) 45–51.
[8] P.R. Harris, H.L. Mobley, G.I. Perez-Perez, M.J. Blaser, P.D. Smith, Gastroenterology 111 (1996) 419–425.
[9] K.A. Eaton, C.L. Brooks, D.R. Morgan, S. Krakowka, Infect. Immun. 59 (1991) 2470–2475.
[10] Zaheer-ul-Haq, A. Wadood, Lett. Drug Des. Discov. 6 (2009) 93–100.
[11] H. Azizian, F. Nabati, A. Sharifi, F. Siavoshi, M. Mahdavi, M. Amanlou, J. Mol. Model. 18 (2012) 2917–2927.
[12] P. Kosikowska, L. Berlicki, Expert Opin. Ther. Pat. 21 (2011) 945–957.
[13] Y. Zhang, J. Feng, Y. Jia, X. Wang, L. Zhang, C. Liu, H. Fang, W. Xu, J. Med. Chem. 54 (2011) 2823–2838.
[14] R. Neelarapu, D.L. Holzle, S. Velaparthi, H. Bai, M. Brunsteiner, S.Y. Blond, P.A. Petukhov, J. Med. Chem. 54 (2011) 4350–4364.
[15] E.M.F. Muri, H. Mishra, S.M. Stein, J.S. Williamson, Lett. Drug Des. Discov. 1 (2004) 30–34.
[16] Zaheer-Ul-Haq, A. Wadood, R. Uddin, J. Enzyme Inhib. Med. Chem. 24 (2009) 272–278.
[17] Z. Rajić, I. Perković, I. Butula, B. Zorc, D. Hadjipavlou-Litina, E. Pontiki, S. Pepeljnjak, I. Kosalec, J. Enzyme Inhib. Med. Chem. 24 (2009) 1179–1187.
[18] R.P. Verma, EXS 103 (2012) 137–176.
[19] M.F. Brown, U. Reilly, J.A. Abramite, J.T. Arcari, R. Oliver, R.A. Barham, Y. Che, J.M. Chen, E.M. Collantes, S.W. Chung, C. Desbonnet, J. Doty, M. Doroski, J.J. Engtrakul, T.M. Harris, M. Huband, J.D. Knafels, K.L. Leach, S. Liu, A. Marfat, A. Marra, E. McElroy, M. Melnick, C.A. Menard, J.I. Montgomery, L. Mullins, M.C. Noe, J. O'Donnell, J. Penzien, M.S. Plummer, L.M. Price, V. Shanmugasundaram, C. Thoma, D.P. Uccello, J.S. Warmus, D.G. Wishka, J. Med. Chem. 55 (2012) 914–923.
[20] W. Guerrant, V. Patil, J.C. Canzoneri, A.K. Oyelere, J. Med. Chem. 55 (2012) 1465–1477.
[21] Z.P. Xiao, X.D. Wang, Z.Y. Peng, S. Huang, P. Yang, Q.S. Li, L.H. Zhou, X.J. Hu, L.J. Wu, Y. Zhou, H.L. Zhu, J. Agric. Food Chem. 60 (2012) 10572–10577.
[22] Z.P. Xiao, D.H. Shi, H.Q. Li, L.N. Zhang, C. Xu, H.L. Zhu, Bioorg. Med. Chem. 15 (2007) 3703–3710.
[23] H.Q. Li, Z.P. Xiao, Y. Luo, T. Yan, P.C. Lv, H.L. Zhu, Eur. J. Med. Chem. 44 (2009) 2246–2251.
[24] Z.P. Xiao, T.W. Ma, W.C. Fu, X.C. Peng, A.H. Zhang, H.L. Zhu, Eur. J. Med. Chem. 45 (2010) 5064–5070.
[25] Z.P. Xiao, Z.Y. Peng, J.J. Dong, J. He, H. Ou-Yang, Y.T. Feng, C.L. Lu, W.Q. Lin, J.X. Wang, Y.P. Xiang, H.L. Zhu, 48 (2013) http://dx.doi.org/10.1016/j.ejmech.2013.03.016.
[26] R. Codd, Coord. Chem. Rev. 252 (2008) 1387–1408.
[27] M.D. Shultz, X. Cao, C.H. Chen, Y.S. Cho, N.R. Davis, J. Eckman, J. Fan, A. Fekete, B. Firestone, J. Flynn, J. Green, J.D. Growney, M. Holmqvist, M. Hsu, D. Jansson, L. Jiang, P. Kwon, G. Liu, F. Lombardo, Q. Lu, D. Majumdar, C. Meta, L. Perez, M. Pu, T. Ramsey, S. Remiszewski, S. Skolnik, M. Traebert, L. Urban, V. Uttamsingh, P. Wang, S. Whitebread, L. Whitehead, Y. Yan-Neale, Y.M. Yao, L. Zhou, P. Atadja, J. Med. Chem. 54 (2011) 4752–4772.
[28] J.H. Kalin, K.V. Butler, T. Akimova, W.W. Hancock, A.P. Kozikowski, J. Med. Chem. 55 (2012) 639–651.
[29] K. Kobashi, J. Hase, K. Uehara, Biochim. Biophys. Acta 65 (1962) 380–383.

[30] N.C. Ha, S.T. Oh, J.Y. Sung, K.A. Cha, M.H. Lee, B.H. Oh, Nat. Struct. Biol. 8 (2001) 505–509.
[31] G.R. Gale, L.M. Atkins, Int. Pharmacodyn. Ther. 180 (1969) 289–298.
[32] K.F. Chan, I.L.K. Wong, J.W.Y. Kan, C.S.W. Yan, L.M.C. Chow, T.H. Chan, J. Med. Chem. 55 (2012) 1999–2014.
[33] Z. Amtul, Atta-ur-Rahman, R.A. Siddiqui, M.I. Choudhary, Curr. Med. Chem. 9 (2002) 1323–1348.
[34] S. Benini, W.R. Rypniewski, K.S. Wilson, S. Mangani, S. Ciurli, J. Am. Chem. Soc. 126 (2004) 3714–3715.
[35] M.W. Weatherburn, Anal. Chem. 39 (1967) 971–974.